AD NUMBER
AD617178
CLASSIFICATION CHANGES
TO: unclassified
FROM: confidential
LIMITATION CHANGES
TO: Approved for public release, distribution unlimited
FROM: Distribution authorized to DoD only; Administrative/Operational Use; JAN 1958. Other requests shall be referred to Armed Forces Special Weapons Project, Sandia Base, Albuquerque, NM.
AUTHORITY
27 Nov 1961 per Defense Atomic Support Agency; 27 Nov 1961 per Defense Atomic Support Agency

CONFIDENTIAL

WT-1148

This document consists of 26 pages

No. 104 of 215 copies, Series A

Operation TEAPOT

NEVADA TEST SITE

February – May 1955

Project 8.4d

SPECTROMETER MEASUREMENTS

Issuance Date: January 27, 1958

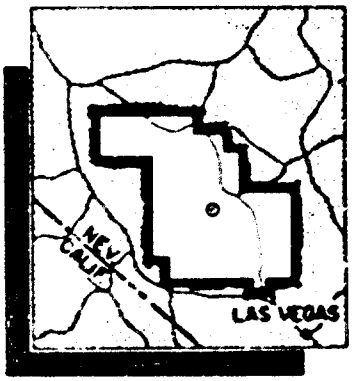

HEADQUARTERS FIELD COMMAND, ARMED FORCES SPECIAL WEAPONS PROJECT
SANDIA BASE, ALBUQUERQUE, NEW MEXICO

WT-1148

OPERATION TEAPOT — PROJECT 8.4d

Report to the Test Director

SPECTROMETER MEASUREMENTS

W.B. Plum
W.J. Parker

U.S. Naval Radiological Defense Laboratory
San Francisco 24, California

SUMMARY OF SHOT DATA, OPERATION TEAPOT

Shot	Code Name	Date	Time*	Area	Type	Latitude and Longitude of Zero Point
1	Wasp	18 February	1400	T-7-4†	762-ft Air	37° 05' 11.6886" 116° 01' 18.7366"
2	Moth	22 February	0545	T-3	300-ft Tower	37° 02' 52.2854" 116° 01' 15.6867"
3	Tesla	1 March	0530	T-9b	300-ft Tower	37° 07' 31.8737" 116° 02' 51.0977"
4	Turk	7 March	0520	T-2	500-ft Tower	37° 06' 18.4644" 116° 07' 03.3679"
5	Hornet	12 March	0520	T-3a	300-ft Tower	37° 02' 26.4643" 116° 01' 31.3674"
6	Bee	22 March	0505	T-7-1a	500-ft Tower	37° 05' 41.3900" 116° 01' 25.5474"
7	ESS	23 March	1230	T-10a	67-ft Underground	37° 10' 00.1283" 116° 02' 37.7010"
8	Apple	29 March	0455	T-4	500-ft Tower	37° 05' 43.0300" 116° 00' 99.0040"
9	Wasp'	29 March	1000	T-7-4‡	740-ft Air	37° 05' 11.6886" 116° 01' 18.7366"
10	HA	6 April	1000	T-5§	36,620-ft MSL Air	37° 01' 43.3643" 116° 03' 20.2254"
11	Post	9 April	0430	T-9c	300-ft Tower	37° 07' 19.6865" 116° 02' 03.8869"
12	MET	15 April	1115	FF	400-ft Tower	36° 47' 52.6387" 115° 55' 44.1000"
13	Apple 2	5 May	0510	T-1	500-ft Tower	36° 03' 11.1006" 116° 06' 09.4037"
14	Zucchini	15 May	0500	T-7-1a	500-ft Tower	37° 05' 41.3900" 116° 01' 25.5474"

* Approximate local time, PST prior to 24 April, PDT after 24 April.
† Actual zero point 36 feet north, 426 feet west of T-7-4.
‡ Actual zero point 94 feet north, 62 feet west of T-7-4.
§ Actual zero point 36 feet south, 397 feet west of T-5.

ABSTRACT

This experiment was performed to obtain data on the spectral distribution of the radiation emitted in a nuclear explosion as a function of altitude. The radiant power versus time was measured with a time resolution of 100μsec in 22 narrow spectral bands between 0.25 and 2.5 microns for the high altitude detonation and for the low altitude correlation shots. This was accomplished with vacuum phototubes and lead sulphide photoconductive cells, each sampling a different spectral region in the focal plane of a medium quartz Hilger spectrograph. The voltages produced by these detectors were recorded on two Ampex Model 306 magnetic-tape recorders.

The spectral distribution at any given instant was obtained by plotting the radiant power per unit wavelength interval as measured by each of these detectors at that time. The spectral distribution is published in this report at the time of the first maximum and at the time of minimum for Shots 1 and 10 and at the time of the second maximum and at several later times for Shots 1, 9, and 10. These spectral distributions indicate that the radiation reaching Building 410 from the high altitude detonation was concentrated more in the shorter wavelengths than for the correlation shots.

This was also a test of the prototype spectrometer, which was designed, fabricated, and operated in too brief a time to achieve optimum performance.

The limited dynamic range of the recorder and the failure of several channels to produce useful data resulted in a deficiency of information between 0.3 and 0.7 microns. The dynamic range can be increased in future spectrometer installations by using more recording channels and alternating them between high and low sensitivity.

FOREWORD

This report presents the final results of one of the 56 projects comprising the Military Effects Program of Operation Teapot, which included 14 test detonations at the Nevada Test Site in 1955.

For overall Teapot military-effects information, the reader is referred to "Summary Report of the Technical Director, Military Effects Program," WT-1153, which includes the following: (1) a description of each detonation including yield, zero-point environment, type of device, ambient atmospheric conditions, etc.; (2) a discussion of project results; (3) a summary of the objectives and results of each project; and (4) a listing of project reports for the Military Effects Program.

PREFACE

The authors wish to express their appreciation of the many helpful suggestions from the other members of the Thermal Radiation Branch of NRDL and from the people contacted at the Naval Ordnance Test Station, China Lake, California and the Naval Electronics Laboratory, San Diego, California. In particular we appreciate the assistance of F. I. Laughridge and J. A. Richardson for their assistance in the design, fabrication, and assembly of the mechanical and electrical components required for the spectrometer.

CONTENTS

Chapter I
INTRODUCTION

1.1 OBJECTIVES

The principal objective of this series of measurements was to determine the spectral distribution of the thermal radiant power from a nuclear detonation achieving a time resolution of approximately 100 μsec. In particular, it was desired to find out if there were any significant differences in spectral distribution between the radiation from a high-altitude air burst and a low-altitude correlation shot. The secondary objective was to test the prototype spectrometer and obtain data which would assist in its further development.

1.2 BACKGROUND AND THEORY

An isothermal sphere expanding by radiative diffusion is formed early in the history of a nuclear explosion, and only the thermal radiation of wavelengths greater than .186 microns has a mean free path of sufficient length to escape into the surrounding atmosphere (Reference 1). A high pressure shock front leaves the surface of this sphere when the temperature has dropped to a level low enough for the velocity of shock propagation to exceed that of the radiative expansion. The advancing shock front generates an opaque layer of heated air which conceals the isothermal sphere and radiates most of the energy contained in the first pulse. This phase ends at breakaway when the shock front is no longer luminous. The second pulse is radiated from the isothermal sphere as the shock heated air becomes transparent.

A decrease in the blast efficiency has been predicted for high altitude detonations on the basis of increased thermal radiation from the shock front (Reference 2). The radius of the fireball at a given temperature is larger for lower ambient densities, and a greater expansion is required to produce the same reduction in temperature. For strong shock conditions the rate of its expansion at a given shock front temperature is the same at both high and low ambient densities. These facts indicate that, if equal increments of temperature are compared as the fireball expands at both high and low altitudes, each increment will be found to last for a longer period of time for lower ambient densities. Since the rate of temperature decline is less at high altitudes, the first pulse lasts for a longer period of time. The thermal radiant power at each temperature is increased because of the larger radiating area. The net result is an increase in the total

energy emitted during the first pulse, thereby consuming energy which would otherwise go into the shock wave. There is nothing in this simplified argument to suggest any significant change in the relative broad band spectral characteristics of the radiation leaving the fireball.

Because of the very-high temperature associated with a nuclear detonation, there is a considerable amount of thermal radiation emitted. This is capable of causing physiological damage due to burns on humans and animals, fires in combustible structures, and a weakening of structural materials because of elevated temperatures. These effects are sensitive to the total energy incident, the rate at which it is delivered, the angles of incidence, and the manner in which it is distributed throughout the spectrum. The latter dependence is due to the variation in absorptivity of all substances with wavelength.

The total thermal radiant power and its spectral distribution at any location must be predicted on the basis of the spectral characteristics of the radiation leaving the surface of the fireball and the effective transmission of the atmosphere. The former quantity depends on the effective temperature and emissivity of the fireball. Since these parameters are not accurately known, the procedure is to measure the spectral distribution at one, or preferably several, distant locations and account for the effect of the atmosphere in extrapolating back to the source. Unfortunately, there are many complicating factors in determining an effective transmission versus wavelength for the atmosphere. These include such factors as a finite-sized fireball in an inhomogeneous atmosphere and instruments with limited fields of view, which also include spectrally selective ground reflections.

A knowledge of the expected spectral distribution of the radiation arriving at a distant location is essential in designing an instrument to measure the total thermal energy or the total thermal radiant power. The absorptivity of the receiving element, the transmission of intervening windows, filters, or lenses, the reflectivity of any mirrors, and any optical magnification must produce a resultant sensitivity that does not vary appreciably over the effective wavelength range of the incident radiation.

The majority of the thermal-radiant-effect studies take place in the laboratory. However, the comparison of laboratory experiments with the corresponding extrapolation of these results to field exposures would be impossible without a detailed knowledge of the spectral distribution of energy, both in the field and in the laboratory.

The majority of the high-speed spectral measurements in the past have been made utilizing photographic techniques and have been made for the determination of phenomena occurring in or around the fireball. The advantage of pulling photographic film through the focal plane of a spectrograph is that the relatively high degree of spectral resolution obtained is required for the identification of atomic and molecular species. For the thermal-effects studies, such high-spectral resolution is generally unnecessary, and the photographic film is not sensitive over the complete wavelength range through which thermal radiant energy is delivered. Quantitative determination of the radiation received is usually simpler and more accurate by making direct photoelectric measurements, rather than by utilising photographic techniques.

Chapter 2

PROCEDURE

2.1 OPERATIONS

The recording spectrometer was located in Building 410, situated near the Control Point area but outside the security fence. The coordinates for this building with reference to the Nevada Survey Grid are:

Elevation: 4,144.25 feet, NSG Easting 678,353.33 feet, and NSG Northing 795,759.48 feet. All of the towers located in the Yucca Flat area were visible from this observation point. The line of sight for the towers in the Frenchman Flat area was intercepted by a mountain range south of the Control Point area.

Although the primary objective was to measure the spectral distribution of the thermal radiant power from Shot 10 and its correlation shots, Shots 1 and 9, data were obtained on Shots 2, 3, 5, 6, 8, and 11. These latter data are not included in this report.

2.2 INSTRUMENTATION

The thermal radiant power as a function of time was measured by various photosensitive detectors in 22 narrow wavelength bands in the interval between 0.25 and 2.5 microns. The center and width of each band, the type of detector, and the instrument in which it was located are given in Table 2.1. A time response of 100μsec was achieved between 0.25 and 1.1 microns by the use of vacuum phototubes. Beyond 1.1 microns the Ektron Detectors lead sulphide photoconductive cells made by Eastman Kodak Company, had a time constant of 200 μsec.

The primary means of wavelength separation was a medium quartz Hilger spectrograph. No pre-slit optics were employed, except for a plane mirror used with the high-altitude detonation. The 5-degree field of view of the spectrograph was large enough to include the entire fireball and the uncertainty of this position on the three air drops. A 16-mm GSAP camera was mounted with its optic axis parallel to the axis of the spectrograph to indicate if the fireball was always within the field of view. The plate-holder assembly was replaced by a housing containing eight phototubes and seven lead sulphide photoconductive cells, each detector sampling a separate spectral region in the focal plane.

The three phototubes at 0.25, 0.29, and 0.35 microns intercepted the radiation directly. Because of the decreasing dispersion, it was necessary to sample the longer-wavelength bands with the aid of mirrors. The lack of sensitivity of the phototubes in the infrared made it necessary to use lead sulphide photoconductive cells beyond 1.1 micron. Since they are temperature and humidity sensitive, they were mounted on a copper block that was temperature controlled, and the unit in which

they were located was desiccated. The radiation calibration was applied to the detectors located in the spectrograph by a 6-volt, 18-ampere, tungsten-ribbon-filament lamp placed in front of the slit a few minutes before shot time.

A secondary system used for wavelength separation was a filter spectrometer containing seven phototubes located behind Baird interference filters. Appropriate blocking filters were used to eliminate the shorter-wavelength pass bands. The phototubes were selected by their threshold wavelengths to exclude the unwanted longer-wavelength radiation.

TABLE 2.1 WAVELENGTH COVERAGE

Wave Length (Microns)	Bandwidth (Microns)	Detector	Instrument
0.25	0.01	RCA 935	Hilger
0.29	0.02	RCA 935	Hilger
0.35	0.05	RCA 935	Hilger
0.35	0.03	RCA 934	Filter Spectrometer
0.45	0.015	RCA 934	Filter Spectrometer
0.49	0.14	RCA 935	Hilger
0.55	0.015	RCA 934	Filter Spectrometer
0.65	0.015	RCA 935	Filter Spectrometer
0.71	0.18	RCA 917	Hilger
0.75	0.015	RCA 926	Filter Spectrometer
0.85	0.10	RCA 917	Hilger
0.85	0.025	RCA 926	Filter Spectrometer
0.95	0.10	RCA 917	Hilger
1.01	0.035	RCA 917	Filter Spectrometer
1.07	0.14	RCA 917	Hilger
1.4	0.035	RCA 917	Hilger
1.7	0.26	Extron Detector	Hilger
2.0	0.23	Extron Detector	Hilger
2.2	0.22	Extron Detector	Hilger
2.4	0.15	Extron Detector	Hilger
2.5	0.16	Extron Detector	Hilger
2.7	0.17	Extron Detector	Hilger

tion. In order to prevent overloading of the tubes, neutral density filters were employed.

The voltages developed by these detectors were recorded on a 1-inch magnetic tape by means of two fourteen-channel Ampex Model 306 magnetic tape recorders having a frequency response essentially flat from direct current to 10 kc/sec. The Model 306 is a frequency-modulated system designed for the recording of transient voltages. A 10-kc timing signal was recorded on one channel. A voltage calibration was automatically applied to all channels at minus 5 seconds. The total recording period lasted for 3 minutes past zero time.

The recorded voltages, later taken off the magnetic tape one channel at a time, were displayed on a Tektronix 531 oscilloscope and photographed by a Polaroid Land camera. This was done for several sweep speeds and deflection sensitivities. The sweep was started just prior to the passing of the first pulse by means of a variable delay trigger circuit activated by an externally magnetized section of the tape 6 feet ahead of the bomb pulse. This latter signal also controlled the opening time of the shutter on the Polaroid Land camera.

The dynamic range of the Ampex Model 306 recorder is only 40 db over the full frequency range of direct current to 10-kc. However, by using low pass electrical filters to restrict the frequency response of

the system to that necessary to accurately reproduce the interesting portion of the pulse on a particular exposure, considerably higher signal-to-noise ratios could be achieved.

A completely overlooked item in the rush of field installation was the shunting effect of long lengths of interconnecting coaxial cable on the load resistance of the phototubes. This was discovered during data reduction, because of abnormally low first-to-second-peak ratios, even on short-wavelength channels. It then became necessary to design a frequency- and phase-correcting network. This was accomplished by developing the playback voltage across an impedance equal to that of the load impedance of the phototube during the recording phase, which was simply the input resistance of the recorder shunted by the capacity of the cable. Since the recording and playback voltages were the same and the impedances were equal, the playback current was equal and in phase with the photocurrent, regardless of frequency. The data voltage was then taken off a much-smaller resistance in series with the playback impedance network. It was only necessary to use this circuit for the first pulse data. The compression of the first pulse served a useful purpose in bringing it within the voltage range of the recorder for Shots 1 and 10, even though the lower irradiance second peak overloaded the recorder.

Chapter 3
RESULTS

Tables 3.1, 3.2, and 3.3 show the useful normalized data from which the spectral distribution curves are determined. The magnetic-tape recorder was overloaded during a portion of the time on the channels at 0.35, 0.49, and 0.85 microns, and the channels at 0.95 micron showed an electrical disturbance which interfered with the first pulse measurements. The channels for which the signal was not measurable above the noise are indicated by dashes. The curves in Figures 3.1, 3.2, 3.3,

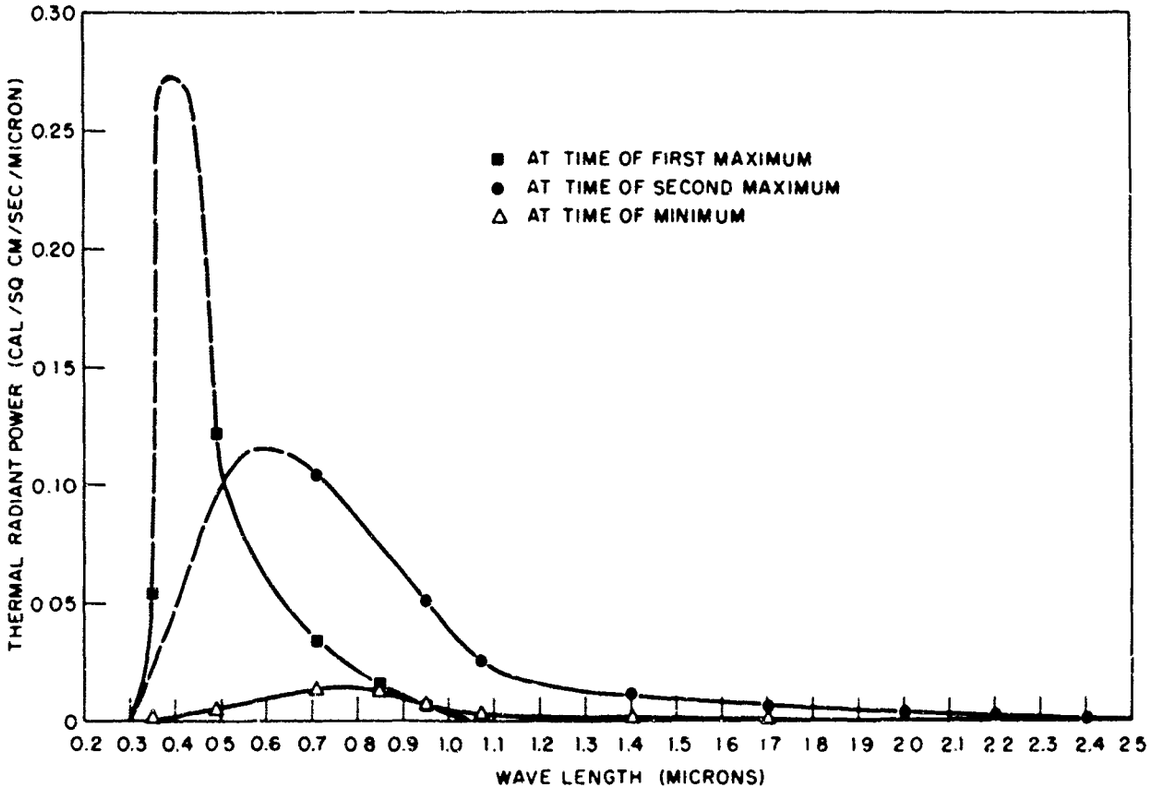

Figure 3.1 Spectral distribution for the maxima and the minimum on Shot 1.

3.4, and 3.5 are drawn according to the procedures outlined in Chapter 4. The spectral distributions shown in Figures 3.2, 3.3, and 3.5 are for times which are one, two, three, and five times the time to the second maximum. There were an insufficient number of points for an exact determination of the dashed portion of each curve. There is a considerable shift of the spectral distribution toward shorter wavelengths for Shot 10 over that for Shots 1 and 9.

TABLE 3.1 SPECTRAL DATA FOR SHOT 1

Thermal Radiant Power (millicalories/ sq cm/sec/micron)

Wave Length (Microns)	First Maximum	First Minimum	Second Maximum 44 m sec	88 m sec	132 m sec	220 m sec
0.35	54	1.4	Overloaded	Overloaded	9.7	7.1
0.49	122	4.4	Overloaded	Overloaded	9.7	20
0.71	34	13	104	71	49	34
0.85	15	12	104	54	40	30
0.95	Interference	6.5	51	36	26	17
1.07	-	1.9	25	16	9	5.1
1.4	-	1.4	11	6.9	4	3
1.7	-	.6	5.8	3.1	2.1	1
2.0	-	-	3.3	2.2	1.9	-
2.2	-	-	1.6	-	-	-
2.4	-	-	0.2	-	-	-

TABLE 3.2 SPECTRAL DATA FOR SHOT 9

Thermal Radiant Power (millicalories/sq cm/sec/micron)

Wavelength (Microns)	Second Maximum 69 m sec	138 m sec	207 m sec
0.35	46	18	10
0.49	254	78	34
0.71	210	77	38
0.85	103	49	28
1.07	40	21	11
1.4	8	5	3
1.7	2	-	-

TABLE 3.3 SPECTRAL DATA FOR SHOT 10

Thermal Radiant Power (millicalories/sq cm/sec/micron)

Wave-Length (Microns)	First Maximum	First Minimum	Second Maximum - 42 m sec	84 m sec	126 m sec	210 m sec
0.35	86	0	Overloaded	Over-loaded	Overloaded	12
0.49	545	66	Overloaded	203	103	51
0.71	160	63	226	144	88	59
0.85	49	43	Overloaded	81	59	36
0.95	Interference	23	90	54	36	22
1.07	-	4	72	40	25	14
1.4	-	3.5	29	19	12	6
1.7	-	2.3	11	6	4	2
2.0	-	1	6	3	2	-
2.2	-	-	3	1.5	1	0.5
2.4	-	-	0.3	0.15	-	-

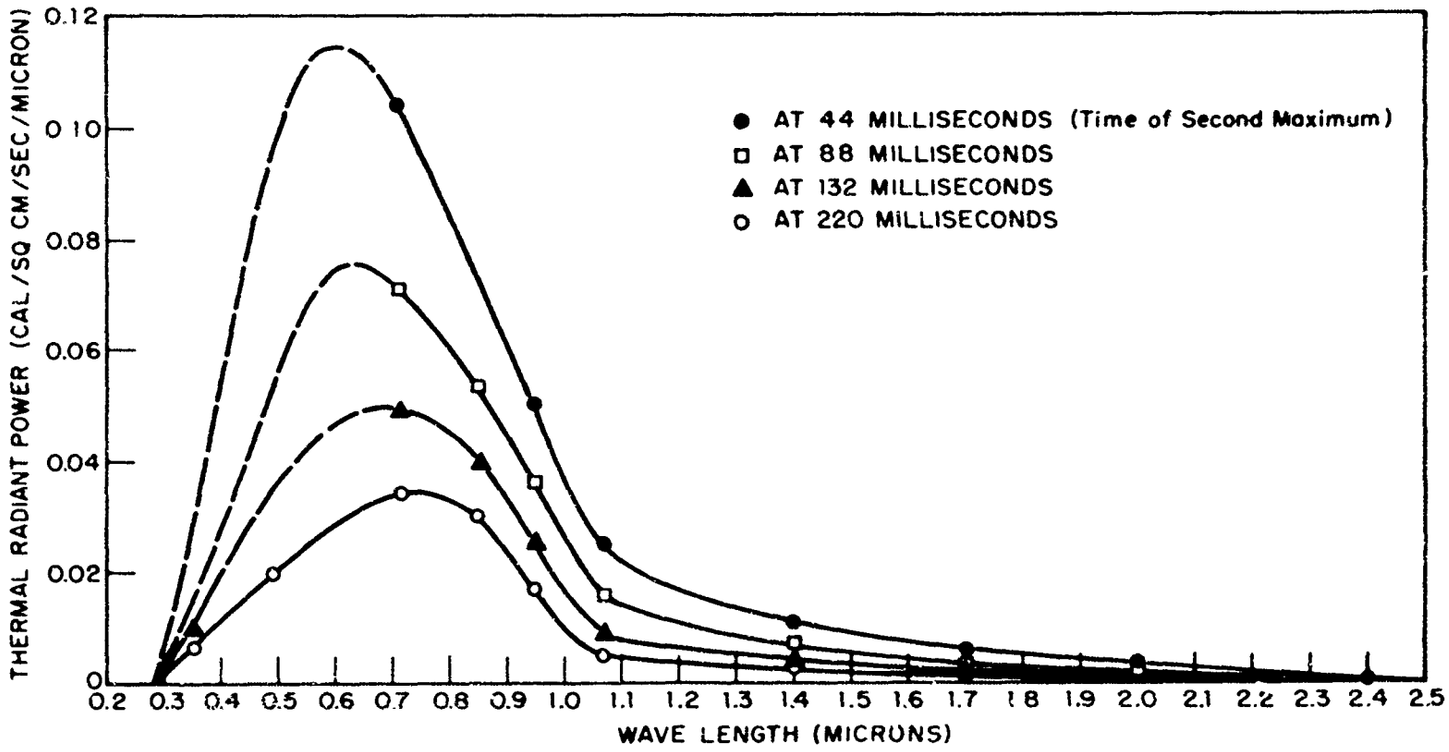

Figure 3.2 Spectral distribution for the second maximum and later times on Shot 1.

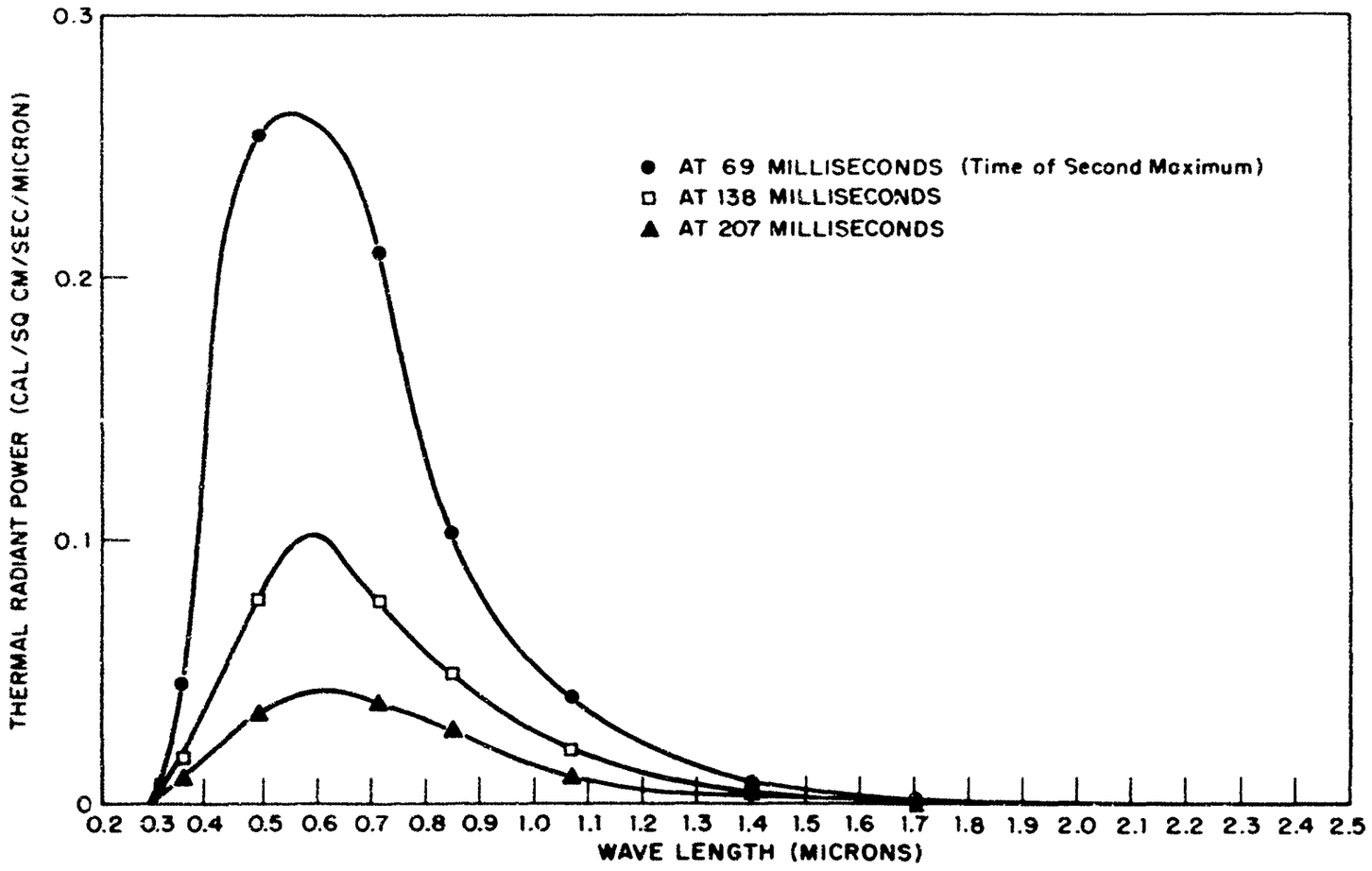

Figure 3.3 Spectral distribution for the second maximum and later times on Shot 9.

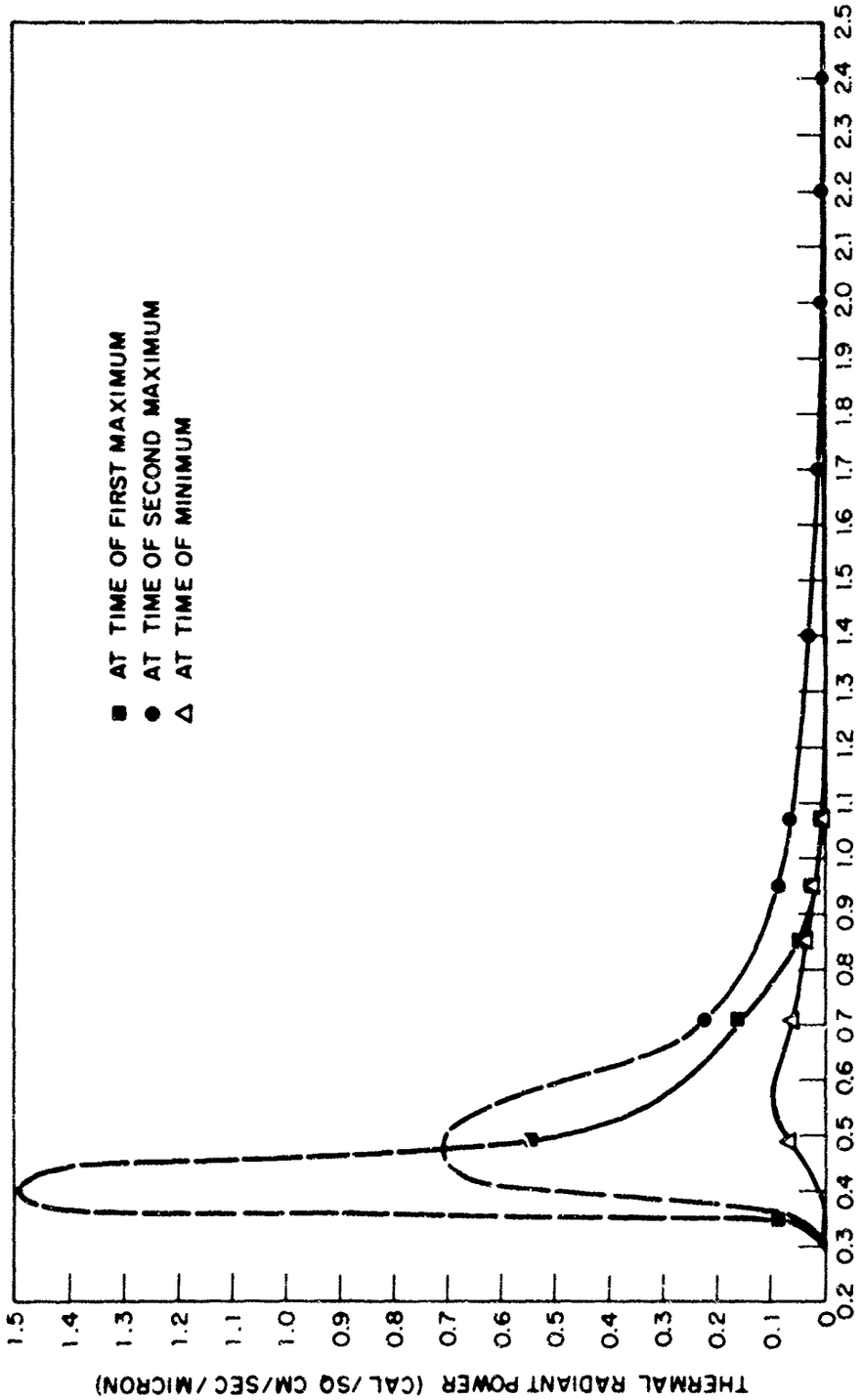

Figure 3.4 Spectral distribution for the maxima and minima on Shot 10.

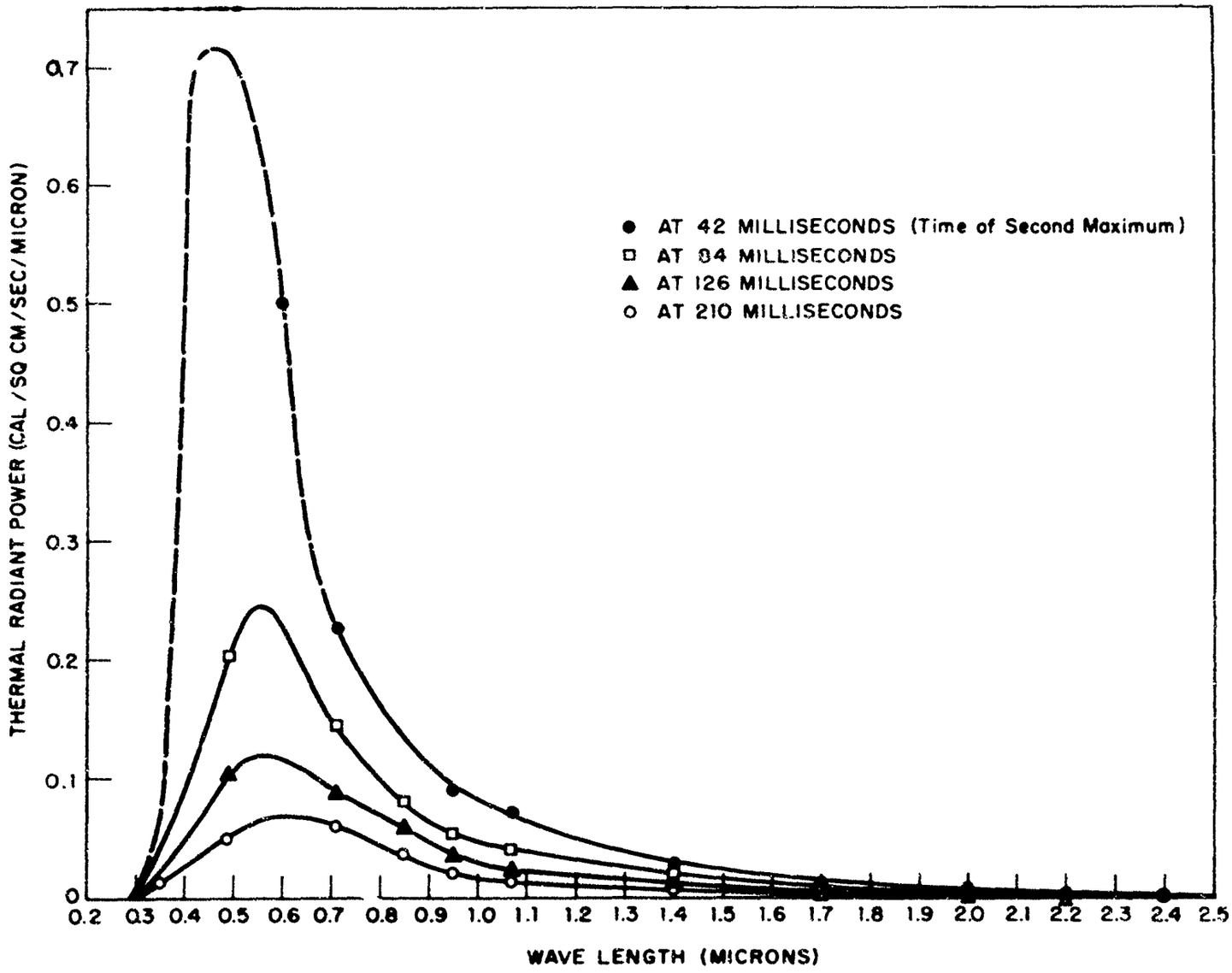

Figure 3.5 Spectral distribution for the second maximum and later times on Shot 10.

Chapter 4

DISCUSSION

The relative calibration factors for the various channels of the spectrometer were determined by placing a tungsten-ribbon filament lamp in front of the slit during a short recording period a few minutes before zero time. The lamp was calibrated by measuring its brightness temperature with an optical pyrometer, correcting for the transmission of the envelope and the emissivity of the filament at 0.665 microns to obtain the true temperature, and then multiplying the Plankian distribution at that temperature by the emissivity values obtained from Reference 3. The absolute units appearing as ordinates in the graphs were found by normalizing the area under the relative spectral-distribution curve to the total radiant power determined by the bolometer (Reference 4) for a particular time during each shot when there were a sufficient number of points to plot a reliable spectral distribution. In fact, the absolute units were determined from an average of these normalizations using the distributions in Figures 3.2, 3.3, and 3.5 at times which were two, three, and five times that of the second maximum.

Unfortunately, the spectral distribution of the second maximum for Shots 1 and 10 could not be obtained directly because three of the critical points were missing due to severe overloading of the magnetic-tape recorder. In order that some indication of the behavior of these curves could be given, they were completed in such a way that the area under the curve was equal to the maximum thermal radiant power as determined from the bolometer (Reference 4). The spectral distributions at the three later times appearing on the same graph give some indication of the possible shape of the distribution curve for the second maximum. In order to make a reasonable shape for the second maximum on Shot 1, it was necessary to assume a maximum thermal radiant power over the entire spectral range measured which was at least 25 percent higher than the published bolometer value. Examination of the raw data from the bolometer does indicate that the second maximum on Shot 1 may be in error by this much. If the error is slightly higher than this, the spectral distribution would have to shift toward shorter wavelengths, and it would resemble more closely the distribution for the other correlation shot, Shot 9, which appeared to peak at a slightly shorter wavelength at the time of second maximum.

Another difficulty that arose at the test site and was discovered too late to be rectified was the loss of time response due to the capacity of the long lengths of interconnecting cables used in the field installation. A system which had 100μsec resolution when tested in the laboratory did not have sufficient response to record the first pulse accurately. A correction network was designed to recover the first pulse data during the process of data reduction. This worked satisfactorily for Shots 1 and 10 where the recorded information was of sufficient amplitude. However, there were an insufficient number of

detectors in the wavelength regions of the first pulse, therefore only points on the base of the pulse were obtained. The first pulse was lost in the noise on Shot 9. This is why no distribution for the first maximum and the minimum were published for that shot.

The data obtained from the filter spectrometer are uninterpretable at this time and are not included in this report. The data at 0.95 microns were not reported for Shot 9, because that channel of the tape recorder was defective. There was an electrical transient that interfered with the measurement of the first maximum at 0.95 microns on both Shots 1 and 10. The loss of the above data made it impossible to draw the distribution for the first maximum accurately. The area under the curve was set equal to the total thermal radiant power over the entire spectral range as measured by the bolometer at that time, but the shape of the curve may be considerably in error.

Because the measurements taken on all shots were made in broad bands in the infrared region of the spectrum, the distributions ignore the structure which must necessarily be there because of atmospheric absorption. No attempt has been made to correct for the atmospheric attenuation in order to determine the spectral distribution of the fireball itself.

Chapter 5
CONCLUSIONS and RECOMMENDATIONS

The results published in this report show that the spectral distribution of the thermal radiation received at Building 410 was concentrated at shorter wavelengths for Shot 10 than for the correlation shots. This may indicate a higher surface temperature for Shot 10, or it may simply be due to different modifying effects of the intervening atmosphere and the underlying terrain. The field of view of the modified Hilger spectrometer included ground reflections on the correlation shots but not on the high altitude detonation. More short-wavelength radiation must have been scattered out from the low-altitude air bursts, because of the longer path length (12.5 miles instead of 9) and because of the haze near the surface.

The modified Hilger spectrometer was a prototype that was conceived, designed, constructed and operated in too short a time to achieve the kind of results that the authors feel such a system is capable of attaining. The limited dynamic range of the recorder and the failure of the filter spectrometer resulted in a deficiency of data between 0.3 and 0.7 microns, which has reduced the reliability of the results. Another instrument of the same general type as the modified Hilger or the filter spectrometer modified to correct the foregoing difficulties and thoroughly laboratory tested before being shipped to the field could be used on another field operation to yield a considerable amount of reliable spectral data, which is really needed for thermal-radiation-effect purposes. It could be calibrated absolutely and, thus also act as a backup for the high-speed bolometer or other fast-time response equipment for measuring total thermal radiant power. If two of these instruments were located at different distances, some measurements of the atmosphere attenuation could be made that could be helpful in extrapolating to other distances. Once this instrument is thoroughly developed and tested in the laboratory, an operator could be trained to obtain reliable data rapidly.

REFERENCES

1. The Effects of Atomic Weapons, (Prepared under the direction of the Los Alamos Scientific Laboratory), M Graw Hill, New York, /50.

2. Shelton, F. H.; High Altitude Effects on Blast-Thermal Partition of Energy from Nuclear Explosions, and Associated Scaling Laws, Sandia Corporation Report No. SC-2969(TR), 15 September 1953, SECRET.

3. DeVos, J. E.; A New Determination of the Emissivity of Tungsten Ribbon, Physica 20, October 1954, page 690-714.

4. Jenkins, R. J., Hopton, R. L., and Plum, W. B.; Irradiance Measurements with High Time Resolution, Operation Teapot, Project 8.4f, WT-1150, CONFIDENTIAL.